











Article

Experimental Characterization of a Microfluidic Device Based on Passive Crossflow Filters for Blood Fractionation

Inês M. Gonçalves ^{1,2,*} , Inês Castro ¹ , Filipe Barbosa ¹ , Vera Faustino ^{1,3,4} , Susana O. Catarino ^{3,4} , Ana Moita ^{2,5} , João M. Miranda ^{6,7} , Graça Minas ^{3,4} , Patrícia C. Sousa ⁸  and Rui Lima ^{1,6,7,*} 

¹ Mechanical Engineering and Resource Sustainability Center (METRICS), University of Minho, 4800-058 Guimarães, Portugal

² IN+, Instituto Superior Técnico, Universidade de Lisboa, 1049-001 Lisboa, Portugal

³ Center for MicroElectromechanical Systems (CMEMS-UMinho), University of Minho, 4800-058 Guimarães, Portugal

⁴ LABBELS—Associate Laboratory, 4710-057 Braga, Portugal

⁵ Centro de Investigação Desenvolvimento e Inovação da Academia Militar, Academia Militar, Instituto Universitário Militar, 1169-203 Lisboa, Portugal

⁶ CEFT—Transport Phenomena Research Center, Faculty of Engineering, University of Porto, 4200-465 Porto, Portugal

⁷ ALiCE—Associate Laboratory in Chemical Engineering, Faculty of Engineering, University of Porto, 4200-465 Porto, Portugal

⁸ INL—International Iberian Nanotechnology Laboratory, 4715-330 Braga, Portugal

* Correspondence: id9385@alunos.uminho.pt (I.M.G.); rl@dem.uminho.pt (R.L.)

Abstract: The separation of red blood cells (RBCs) from blood plasma and the analysis of individual RBCs are of great importance, as they provide valuable information regarding the health of their donor. Recent developments in microfluidics and microfabrication have contributed to the fabrication of microsystems with complex features to promote the separation and analysis of RBCs. In this work, the separation capacity of a multi-step crossflow microfluidic device was evaluated by using a blood analogue fluid made by Brij L4 micelles and human RBCs separated from whole blood, suspended in a solution with hematocrits (Ht) of 0.5 and 1%. All the samples collected at the outlets of the device were experimentally analyzed and compared. The absorbance spectrum was also measured for the prepared blood samples. The results indicate that the tested blood analogue fluid has exhibited a flow behavior similar to that of blood. In addition, the optical absorbance spectrophotometry revealed that it was possible to evaluate the separation efficiency of the microfluidic device, concluding that the concentration of cells was lower at the most lateral outside outlets of the microchannel due to the cumulative effect of the multiple cross-flow filters.

Keywords: blood on chip; blood analogue; cell separation; passive microfluidic device; crossflow microfluidic device; optical absorbance spectrophotometry



Citation: Gonçalves, I.M.; Castro, I.; Barbosa, F.; Faustino, V.; Catarino, S.O.; Moita, A.; Miranda, J.M.; Minas, G.; Sousa, P.C.; Lima, R. Experimental Characterization of a Microfluidic Device Based on Passive Crossflow Filters for Blood Fractionation. *Processes* **2022**, *10*, 2698. <https://doi.org/10.3390/pr10122698>

Academic Editors: Yanzhen Zhang and Tao Sun

Received: 22 October 2022

Accepted: 9 December 2022

Published: 14 December 2022

Publisher's Note: MDPI stays neutral with regard to jurisdictional claims in published maps and institutional affiliations.



Copyright: © 2022 by the authors. Licensee MDPI, Basel, Switzerland. This article is an open access article distributed under the terms and conditions of the Creative Commons Attribution (CC BY) license (<https://creativecommons.org/licenses/by/4.0/>).

1. Introduction

One of the most widely used applications of microfluidic devices is the separation of microparticles and blood cells according to their physical and mechanical properties, such as size, shape, deformability, and density [1–3]. Such devices can be of great importance as they can be used as a diagnostic and prognostic tool for blood diseases. For instance, they have the ability to isolate key components from a blood sample that correlate to a specific pathological condition. This approach enables accurate diagnostics with small biological samples taken from the patient [4,5].

According to the manipulating forces, microfluidic systems that perform blood plasma separation can be categorized as active or passive types [3,4]. The active approach requires an external force field, whereas the passive approach depends entirely on geometrical effects and nonlinear hydrodynamic forces [3,4,6,7]. Due to their simpler mechanisms and low fabrication costs, these latter methods have gained continuous interest within the microfluidic research community. For instance, Karimi et al. [8] have used physical

filtration microstructures (pillar-type filters) to perform blood cell separation. However, by using this method, problems such as clogging and jamming are likely to arise within the microfluidic device [3,9]. To minimize such problems, several microfluidic systems having crossflow filters were developed [5,10–14]. By using this approach, the micelles/cells flow tangentially along the pillars, in contrast with the classical filtration approaches, where they flow through the pillars of the filter. For instance, Rodrigues et al. [12] have developed a device having crossflow filters to perform blood cell separation and hyperbolic contractions to assess cell deformability. Later, Faustino et al. [5,13,14] used upgraded microfluidic devices to evaluate the ability to separate healthy and rigid blood cells.

Human blood is a complex biofluid that has important biological components and can be used in *in vitro* tests to diagnose different kinds of pathologies. Therefore, the separation of the plasma and its several components (RBCs, white blood cells, and platelets) using a single microfluidic device can contribute to new ways to detect and diagnose blood diseases [15,16]. Nevertheless, there are several complex challenges regarding the use of real blood in microchannels that must be overcome, such as sample storage, sedimentation, coagulation, and consequent blockage of the micropillars [17]. Hence, blood analogues are gaining popularity among biomedical researchers as this fluid is much easier and safer to prepare, handle, and store [17,18]. In recent years, several successful blood analogues have been developed by different techniques such as flow focusing, two-syringe membrane emulsification, and multi-stage membrane emulsification [17–20]. However, Lima et al. [21] have recently developed an extremely simple blood analogue made of Brij L4 surfactant micelles suspended in pure water.

This work is part of a larger project that aims to create an innovative microfluidic device to perform simultaneous partial cell separation and cell analysis. The main objective of this device is not to completely separate the cells from the serum but to partially separate the cells (with different degrees of effectiveness) in order to lower the hematocrit at the outlets and in this way to assess individual cells' deformability. It should be noted that high hematocrit (Ht) samples at the outlet do not allow cell deformability assessment by means of a high-speed video microscopy system. This work presents, for the first time, an experimental flow study on the separation efficiency of a continuous and high-throughput microfluidic device with several crossflow filters and bifurcations by using both Brij L4 blood analogue fluid (BAF) and *in vitro* blood at different Ht values. In addition, optical absorption spectrophotometry was used to evaluate the partial separation degree throughout the device. To our knowledge, the evaluation of the separation of RBCs from the plasma, its comparison to an analogue fluid, and the use of absorbance measurements for separation quantification have not yet been performed on this type of microfluidic device, which enhances the novelty of this work and opens new possibilities regarding the development of separation devices for biofluids. Thus, our device can be employed for both the analysis of the cells' deformability and continuous partial separation.

2. Methods

2.1. Microchannel Design and Fabrication

A PDMS microfluidic device was manufactured by soft lithography using SU-8 (Microchem Corp., Newton, MA, USA) molds, as extensively reported in [3,18]. In brief, the PDMS silicone elastomer kit, Sylgard™ 184 from Dow Corning (Midland, MI, USA), was prepared according to the manufacturer's instructions by mixing the pre-polymer with the respective curing agent at a ratio of 10:1. The mixture was then poured onto the mold and left for 2 h at 70 °C in an oven for curing. Lastly, the microchannel was removed from the mold and adhered to a clean glass surface using oxygen plasma. A hole puncher (Elveflow, Paris, France) was used to create both inlet and outlet ports in the PDMS microfluidic device before its adhesion to the glass slide.

Regarding the microchannel design, it presents one inlet and nine outlets. In particular, it exhibits a straight microchannel after the inlet with ramifications at approximately $\frac{1}{4}$ of its length from the inlet. Each outlet has a mirror outlet on the other side, with the exception

of the one furthest away from the inlet, O5. The geometry and respective main dimensions are presented in Figure 1 and Table 1. The device presents three filtering regions in series, on each side of the microdevice, comprised of arrays of pillars, and it is through these features that the central channel connects with the side channels. Outlets O3 and O7 collect the retentate of separation step 2, outlets O2 and O8 collect the retentate of separation step 2, and, finally, outlets O1 and O9 collect permeate of the separation step 3. Outlets O4, O5, and O6 follow collect the retentate from separation step 1, which flows along the main channel. These features promote the crossflow, so the micelles/cells are induced to remain in the central channel while the fluid is distributed between all the channels. The presence of hyperbolic contractions before all outlets (except O5), although not affecting the separation efficiency of the micro-structure, is essential to control the flow velocity and the passage of the micelles and cells to those exits, allowing for the individual cells' mechanical characterization [5].

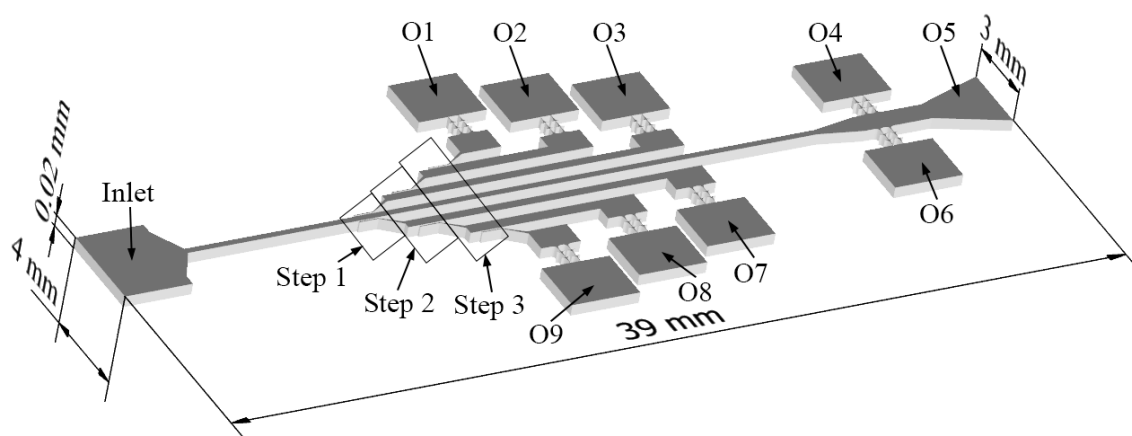
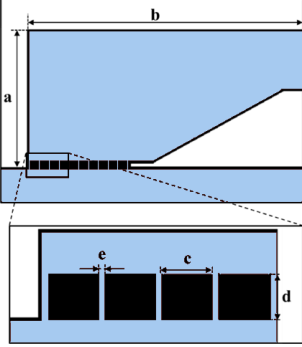
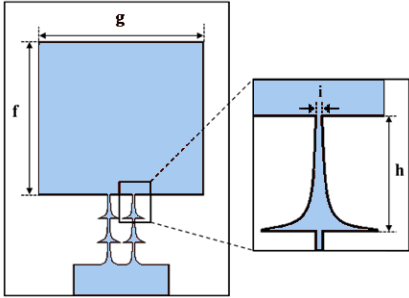


Figure 1. Schematic diagram of the geometry and dimensions of the tested multi-step crossflow microfluidic device. The device has one inlet and nine outlets (O1 to O9). At approximately $\frac{1}{4}$ of its length, the main channel connects with the lateral channels on both sides through ramifications with a row of pillars (steps). Hyperbolic constrictions are present before each outlet, with the exception of outlet 5. The main channel has a width of 0.5 mm and the side channels have a width of 0.4 mm after the first separation step and 0.5 mm after the following step.

2.2. Blood and Blood Analogue Samples

The initial studies were performed using a BAF. The analogue was prepared using the surfactant Brij L4 (Merk, Darmstadt, Germany) mixed in distilled water in a proportion of 1% *w/w*. The mixture was then stirred manually for 1 min, to promote the formation of micelles of the surfactant. The emulsion was then pushed through a filter, with an average pore size of 20 μm , in a precolumn. Consequently, the size and shape of the micelles became more uniform. A schematic representation of the manufacture and visualization of the analogue fluid is presented in Figure 2. Despite the size difference, the Brij L4 analogue has not only a similar behavior to the RBCs' deformability but also presents a similar rheology in comparison to *in vitro* blood [21].

Table 1. Main dimensions of the multi-step crossflow microfluidic device.

Microfluidic Device			
	Step 1	a = 830 μm b = 1030 μm	c = 55 μm d = 50 μm e = 10 μm
	Step 2	a = 830 μm b = 1030 μm	c = 55 μm d = 50 μm e = 10 μm
	Step 3	a = 830 μm b = 1030 μm	c = 55 μm d = 50 μm e = 10 μm
Hyperbolic Constrictions			
			f = 2500 μm g = 3000 μm h = 318.8 μm i = 19.9 μm

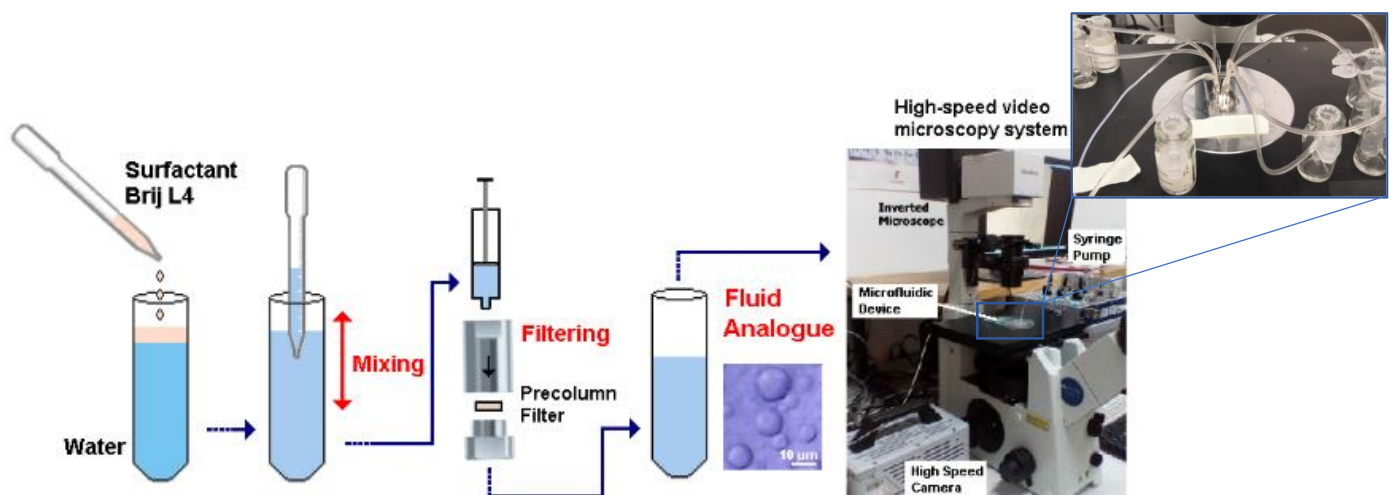


Figure 2. Schematic representation of the preparation and visualization of the blood analogue fluid. The surfactant is mixed with water to form micelles. Then, the solution is filtered to uniformly size the micelles. Finally, the fluid is loaded onto the syringe pump connected to the microfluidic device, and the flow is visualized and acquired through a high-speed camera connected to an inverted microscope.

In a second phase, the experimental assays were performed using solutions with different concentrations of human RBCs, collected from whole blood provided by healthy individuals to the Instituto Português do Sangue e da Transplantação—IPST (Portuguese Institute of Blood and Transplant). To prepare the samples, RBCs were separated from whole blood by centrifugation: the whole blood was centrifuged at 6000 rpm for 10–15 min and washed three times with $1 \times$ PBS. The plasma, as well as the white blood cells, were

discarded. The RBCs were added to a 5 wt.% Dextran 40 (40,000 mol wt., Thermo Fisher Scientific, Waltham, MA, USA) solution to achieve a hematocrit of 0.5 or 1%.

2.3. Experimental Setup

For the microfluidic assays, a syringe pump (NEMESYS, CETONI, Korbußen, Germany) was connected to the microfluidic devices for pumping, and a flow rate of 50 and 100 $\mu\text{L}/\text{min}$ was defined for the blood analogue and human red blood cell samples, respectively. The flow was visualized using a high-speed camera (Fastcam SA3, Photron, Motion Engineering Company, Westfield, IN, USA) connected to an inverted microscope (IX71; Olympus Corporation, Tokyo, Japan), at a frame rate of 2000 frames/s and a shutter speed ratio of 1/75,000.

The fluids were collected from the nine outlets during 5 min of continuous perfusion through the microchannel, as presented in Figure 3, and collected into 2.5 mL volume test tubes. Then, the samples were evaluated regarding the amount of volume exiting through each outlet and collected by each tube. That volume is shown as the percentage of the test tube's capacity that was filled by the collected fluid, so a volume of 100% corresponds to the full volume of the test tube.

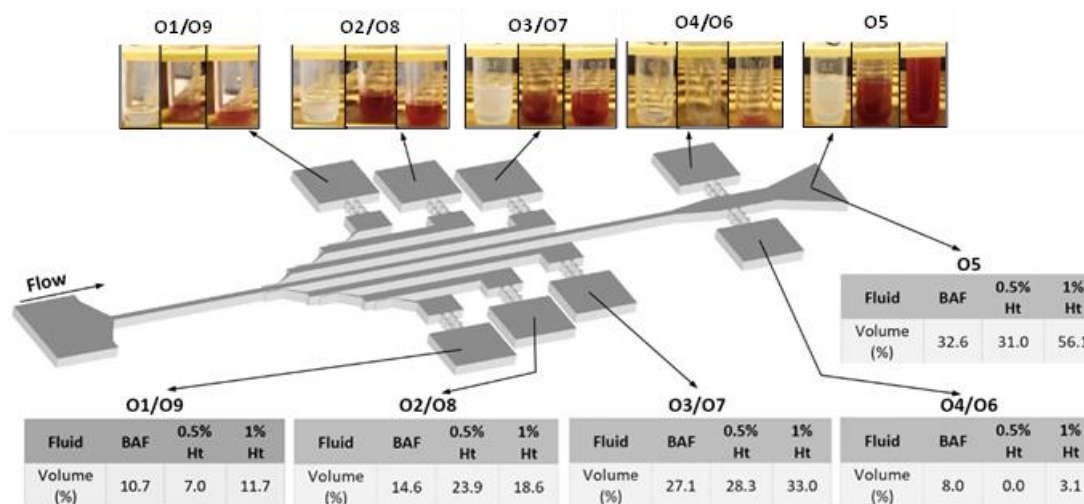


Figure 3. Representative samples of all the fluids collected at the outlets of the channel for quantitative and qualitative studies. The tested fluids were a blood analogue fluid (BAF) made by Brij L4 micelles and a solution prepared from human blood samples with hematocrits (Ht) of 0.5 and 1%. The volume collected is presented as the percentage of a test tube capacity that was filled.

2.4. Optical Characterization

To evaluate the separation efficiency and distinguish the fluid collected from each outlet, the differences in the hemoglobin concentration between the samples were evaluated through optical absorbance spectrophotometry. For that purpose, a quartz tungsten halogen light source of 200 W (model 66881, Oriel Newport, Stratford, CT, USA), optic fiber absorption probes, a cuvette to support the samples, and an AvaSpec-ULS2048XL EVO spectrophotometer with an integrated monochromator (Avantes, Ns Apeldoorn, The Netherlands) were used [22,23]. The transmittance (T) of the samples was calculated by the equipment software according to Equation (1).

$$T = \frac{I}{I_0} \quad (1)$$

where I is the intensity of the light transmitted by the sample, and I_0 is the intensity of the light applied to the sample (measured using a reference sample). The absorbance (A) is

then calculated using the obtained transmittance values, according to the Lambert-Beer law, Equation (2) [13].

$$A = \log_{10}(T) \quad (2)$$

The separation efficiency, when using the BAF, was evaluated by analyzing the recordings of the flow at the inlet and at each outlet, through the software ImageJ. Each recording was converted to a single image by applying the average intensity and using the Z Project function. The intensity of the pixels in the region of interest was obtained using the Plot Profile function. An example of the obtained measurements is displayed in Figure 4. The intensity values could vary from 0 to 255, with black being 0 and white being 255. The zero values, which can be seen in Figure 4, correspond to the microchannel walls, whereas the region of interest is between them. A normalization process was applied in each frame to remove the effect from the walls. At least three measurements were performed in each region of interest, and the average for each region was then calculated and compared.

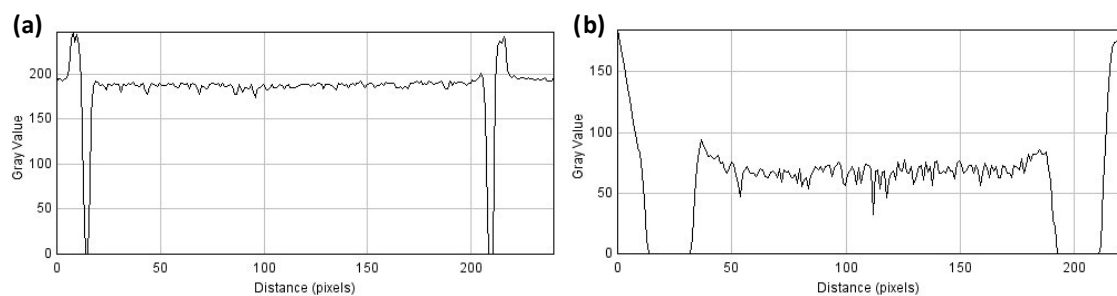


Figure 4. Plot profile obtained from the recordings of the BAF flow through the microchannel at the (a) inlet and (b) outlet one/nine using the software ImageJ (1.48 v). The zero value indicates a black pixel, which corresponds to the channel walls. Consequently, the values between those points were the ones considered for the average calculation.

3. Results and Discussion

3.1. Fluid Volume

The amount of fluid that exits the microchannels varies among the outlets of the channel but is similar between mirror outlets. Figure 5 presents the percentage of fluid collected at the outlets of the microchannel after 5 min of continuous flow.

The outlet where a greater volume of BFA was collected was outlet five, followed by outlet three and its respective mirror outlet, O7. Outlets one and two, and respective mirror outlets, had low amounts of analogue fluid exiting through them, with O2 and O8 having a slightly higher volume than O1 and O9. Outlets four and six had little to no volume exiting through them. It was also noticeable that the fluid was more transparent at outlets one and two, enhancing the lower quantity of micelles collected at these outlets.

As expected, the several ramifications of the channels, together with the pillars and hyperbolic constrictions, made the path difficult for the micelles and, consequently, the fluid, so they exit mainly through O5. In addition, the pillars and contractions can contribute to the accumulation of residues and micelles, hindering the exit through the lateral outlets.

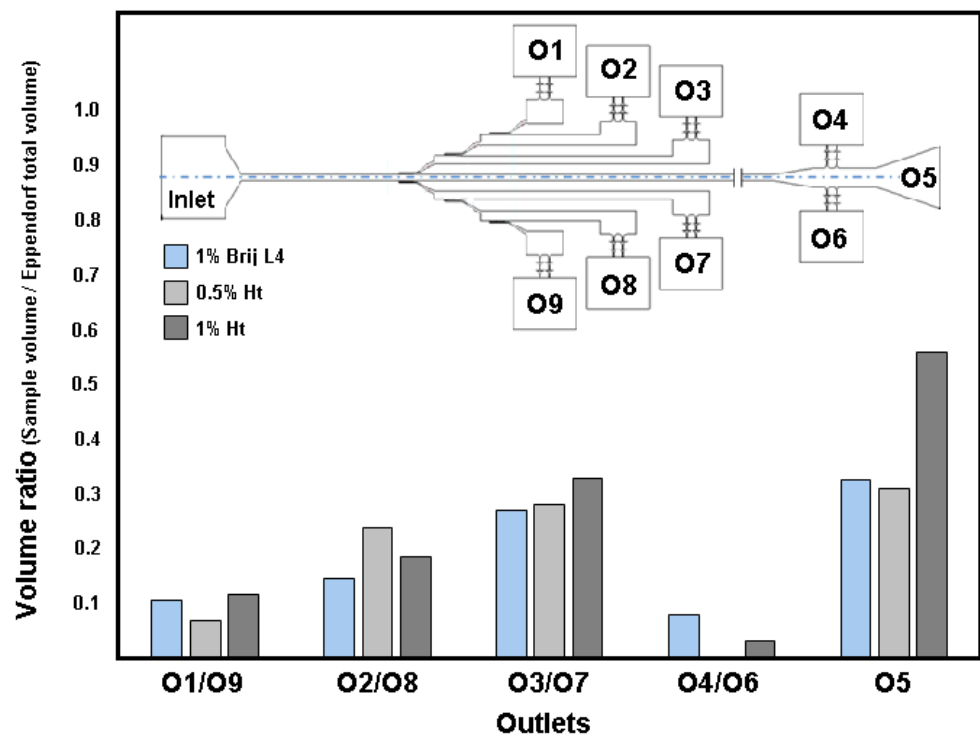


Figure 5. Percentage of fluid collected from the channel after 5 min of continuous flow of Brij L4 BAF and Dextran 40 with 0.5% and 1% Ht for a maximum of 2.5 mL.

The particle separation capability of the microchannels was then evaluated using healthy human RBCs in Dextran 40, at a hematocrit of 0.5 and 1%. When using the solution with RBCs, the behavior registered at the outlets was similar to that observed when using analogue fluids. There is an increasing volume of fluid exiting the channel from outlets 1 to 3 and their respective mirror outlets. Outlet 5 resulted in the most volume of fluid exiting, while little to no volume of fluid exited through O4 and O6.

Overall, similar volumes were collected from each outlet of the microchannel when using the analogue fluid and the fluids with RBCs. In addition, for all the fluids, the samples collected from O5 seemed to present a greater concentration of cells or micelles than the samples collected from O1 and O9. Consequently, the analogue fluid showed potential as a good tool to replace the use of blood when evaluating the separation between cells and fluid on microfluidic channels. However, strategies for the quantification of the amount of micelles collected at the outlets when using analogue fluids should be considered in future investigations for a more accurate comparison with biological fluids.

3.2. Absorbance

To compare the amount of hemoglobin that exited the channels through each outlet, the absorbance spectrum of the samples in each outlet was acquired. As it can be seen in Figure 6, the blood absorbance spectrum is most relevant between the wavelengths of 350 and 750 nm, with the highest absorbance peak at 412 nm [24]. The higher the peak at that wavelength, the higher the amount of hemoglobin in the sample.

The first measurements of absorbance were performed on the original 0.5% and 1% Ht samples to establish a spectral reference for the amount of hemoglobin in the microchannel inlet. As it can be seen in Figure 7, both samples have an absorbance peak around 412 nm, which is in agreement with the literature [25]. Additionally, as expected, the solution with 1% Ht presents higher values of absorbance since it contains twice the hemoglobin as the 0.5% Ht solution.

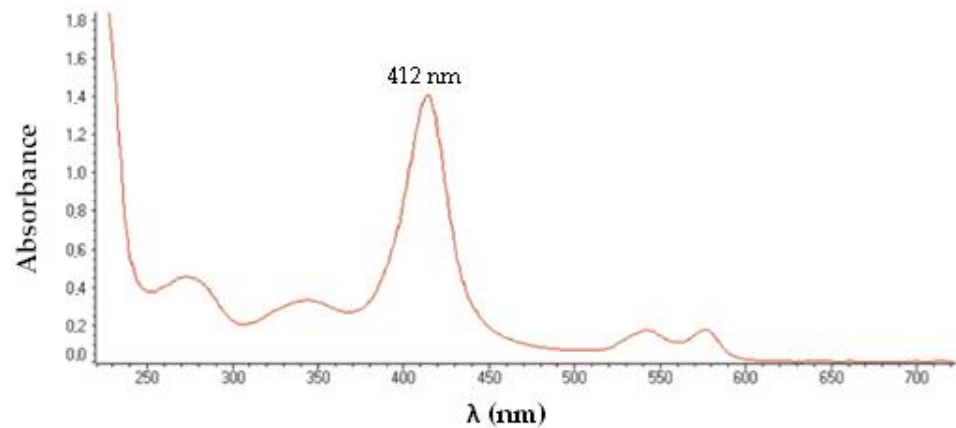


Figure 6. Standard UV-Visible absorbance spectrum (a.u.) of RBCs diluted in distilled water, in the 230–720 nm wavelength (λ , nm) range of the optical spectrum. The maximum absorbance value was registered at 412 nm. Adapted from [26], under the terms of the Creative Commons Attribution License.

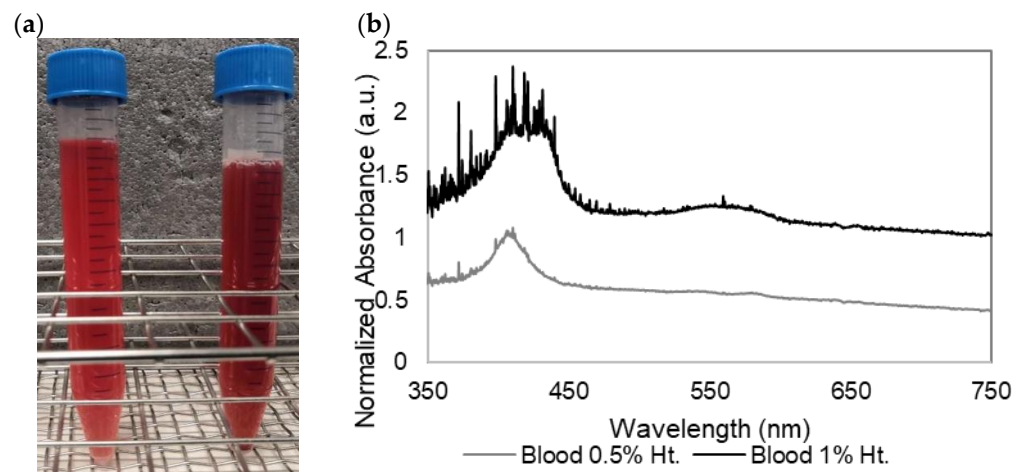


Figure 7. (a) Samples of RBCs in Dextran 40 at a hematocrit of 0.5%, on the left, and 1%, on the right, used in this study, and respective (b) normalized absorbance spectra (a.u.) in the 350–750 nm optical range.

The absorbance of the samples collected at the outlets of the channel for both fluids with RBCs was calculated, and the results are presented in Figure 8. It should be noted that the samples obtained at outlets four and six did not present a sufficient amount of fluid for the measurement to be performed, and so no optical data was acquired.

For the fluid with 0.5% Ht, the peak at 412 nm is higher for O5, with values close to the ones at the inlet. On the other hand, the peak is smaller at O1 and O9, indicating a lower amount of hemoglobin (as a result of a lower number of RBCs in those outlets) in those samples. For the fluid with 1% Ht, the peak is also smaller for O1 and O9. The remaining outlets present very close values between them, being slightly higher at O5 and lower at O3 and O7, which indicates that the resolution of the system is not high enough to detect the variations from those samples.

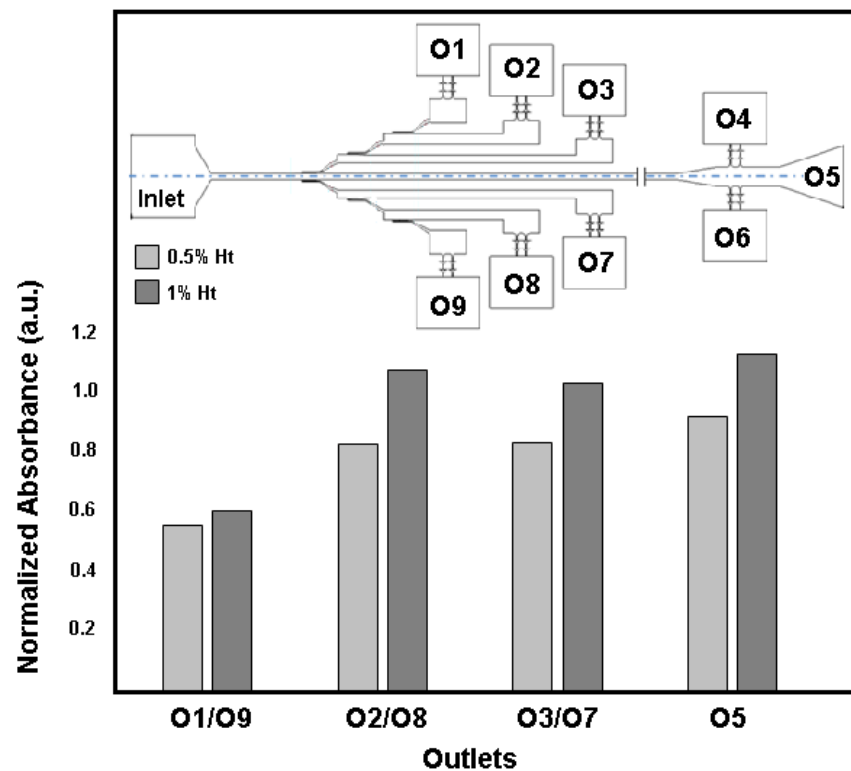


Figure 8. Normalized absorbance spectrum (a.u.) at 412 nm of the samples in the inlet and collected from the outlets of the microchannel using 0.5% Ht and 1% Ht.

3.3. ImageJ Analysis

The average gray intensity of the regions near the inlet and outlets is shown in Figure 9. The highest value was obtained at the inlet, while the smallest value was obtained at outlets one and nine, as expected. The value also gradually increases from O1/O9 to O5. Considering that the particles presented a whitish coloration, a greater concentration of particles would lead to an image with a lighter pixel and, consequently, a gray value closer to 255. The inlet presents a greater gray average value since it is the region with higher particle concentration. According to the results obtained for the blood samples, there are fewer particles exiting through O1/O9 than through O5. Consequently, the results allow us to conclude that the developed BAF behavior is similar to that of human blood on this type of microfluidic device.

Although the results are promising and corroborate the ones obtained by absorbance spectrophotometry with the blood samples, it is important to notice that, since this evaluation can be influenced by many factors related to the image acquisition (such as image intensity or frame rate acquisition), future work should also consider the use of other measurement techniques to improve the quantification of micelles present at each outlet.

Considering the obtained results, a partial and continuous separation was observed between the micelles and cells, as well as the fluid. For all the tested fluids, greater volumes were collected at the outlet straight across the inlet, O5, and those samples presented a dark coloration. On the other hand, the samples collected from O1 and O9 presented a lighter coloration, and, from the absorbance studies, it was verified that the amount of RBCs was much lower than the amount at the inlet, meaning that, in fact, the sequence of three cross-flow separation levels is the one that assures a better separation of the cells from plasma.

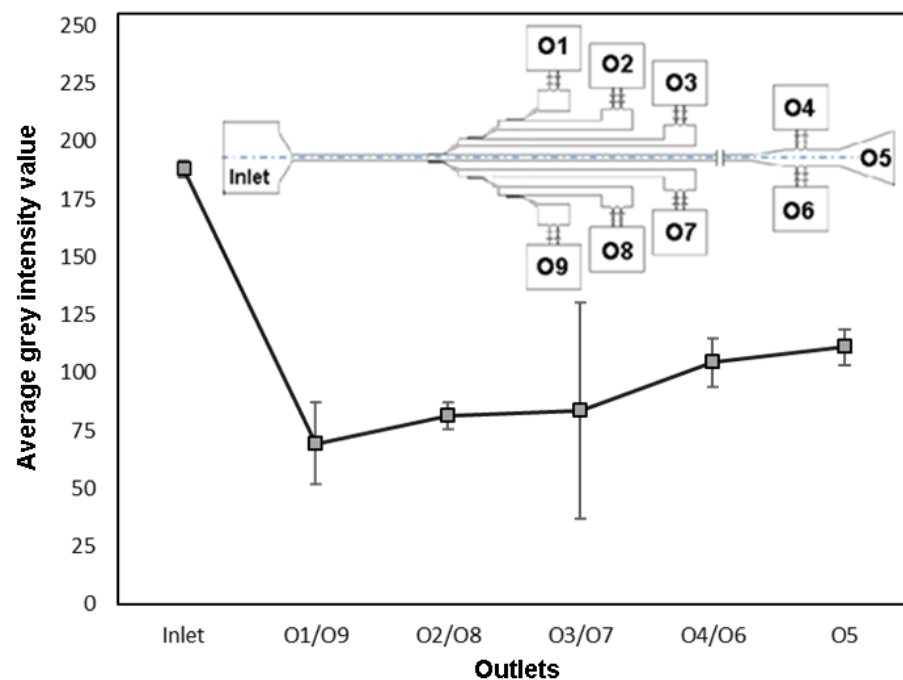


Figure 9. Average gray intensity value (a.u., ranging from 0 to 255) at the inlet and 9 outlets of the microfluidic device.

4. Conclusions and Future Works

In this study, we have assessed the separation of micelles and cells from a fluid on a multi-step cross-flow microfluidic device. The tested device exhibited the ability to separate RBCs and Brij L4 micelles from the base fluid. The separation was possible due to crossflow filters that have served as barriers for the passage of the micelles and RBCs. However, further optimizations of the geometry of the microchannel should be considered in future studies. Lastly, the incorporation of deformation studies as well as biochemical analyzes could also be considered once the optimization of the channel is complete. The developed device has the potential to be incorporated on a lab-on-a-chip device and, consequently, be used to separate and evaluate blood components in a fast and continuous way with a small amount of sample. The processing of blood samples, including the separation of cells from serum, is currently required by medical devices for blood analysis. This is typically performed through centrifugation, which entails greater expenditures and top-bench centrifuge equipment, as well as a greater risk of harming the cells. By enabling a continuous and passive partial separation of the cells from the plasma, this microfluidic device overcomes the drawbacks of current commercial devices and ensures quick processing of blood samples with different hematocrit levels at various outlets. As a result, there is a significant chance that this technology will be applied to the medical industry, either for characterizing cells or even for coupling to more modern blood analysis devices, eliminating the need for larger and more expensive equipment.

The blood analogue used in this study has shown similar behavior to that observed when using the physiologic fluid. This reinforces the usefulness of this blood-analogue fluid as a substitute for blood in preliminary tests of microfluidic devices, minimizing the use of whole blood. Accessing whole blood from human donors can be difficult, and the protocols required are more complex. However, methods to quantify the BAF microparticles should be explored in future work to better evaluate and compare the separation occurring in microfluidic devices. Future research should also look into blood analogue fluids that mimic certain pathologic conditions that affect the blood cells, such as RBCs rigidity.

Author Contributions: Conceptualization, V.F., R.L., S.O.C. and G.M.; methodology, I.M.G., I.C., S.O.C. and P.C.S.; validation, I.M.G., I.C., S.O.C., P.C.S., G.M. and R.L.; formal analysis, I.M.G. and I.C.; investigation, I.M.G., I.C., V.F., R.L. and S.O.C.; resources P.C.S., G.M. and R.L.; data curation, I.M.G., I.C., R.L. and S.O.C.; writing—original draft preparation, I.M.G., F.B., V.F., S.O.C., A.M., J.M.M., P.C.S., G.M. and R.L.; writing—review and editing, I.M.G., F.B., V.F., S.O.C., A.M., J.M.M., P.C.S., G.M. and R.L.; supervision, P.C.S., A.M. and R.L.; funding acquisition, P.C.S., G.M. and R.L. All authors have read and agreed to the published version of the manuscript.

Funding: This research was funded by the Fundação da Ciência e da Tecnologia (FCT), under projects PTDC/EEI-EEE/2846/2021 and EXPL/EME-EME/0732/2021, and national funds (OE), within the scope of the Scientific Research and Technological Development Projects (IC&DT) program in all scientific domains (PTDC, EXPL), through the FCT, I.P. The research was also supported by LA/P/0045/2020 (ALiCE), UIDB/00532/2020, UIDP/00532/2020 (CEFT), UIDB/04077/2020, UIDB/04436/2020, and national funds through FCT/MCTES (PIDDAC).

Data Availability Statement: The data presented in this study are available upon reasonable request.

Acknowledgments: Inês M. Gonçalves acknowledges the PhD scholarship BD/08646/2020 attributed by FCT. S.O.C. thanks FCT for her contract funding provided through 2020.00215.CEECIND.

Conflicts of Interest: The authors declare no conflict of interest.

References

- Zhang, J.; Yan, S.; Yuan, D.; Alici, G.; Nguyen, N.T.; Ebrahimi Warkiani, M.; Li, W. Fundamentals and applications of inertial microfluidics: A review. *Lab Chip* **2016**, *16*, 10–34. [[CrossRef](#)] [[PubMed](#)]
- Nasiri, R.; Shamloo, A.; Ahadian, S.; Amirifar, L.; Akbari, J.; Goudie, M.J.; Lee, K.; Ashammakhi, N.; Dokmeci, M.R.; Di Carlo, D.; et al. Microfluidic-Based Approaches in Targeted Cell/Particle Separation Based on Physical Properties: Fundamentals and Applications. *Small* **2020**, *16*, 2000171. [[CrossRef](#)] [[PubMed](#)]
- Catarino, S.O.; Rodrigues, R.O.; Pinho, D.; Miranda, J.M.; Minas, G.; Lima, R. Blood Cells Separation and Sorting Techniques of Passive Microfluidic Devices: From Fabrication to Applications. *Micromachines* **2019**, *10*, 593. [[CrossRef](#)] [[PubMed](#)]
- Wyatt Shields Iv, C.; Reyes, C.D.; López, G.P. Microfluidic cell sorting: A review of the advances in the separation of cells from debulking to rare cell isolation. *Lab Chip* **2015**, *15*, 1230–1249. [[CrossRef](#)]
- Pinho, D.; Faustino, V.; Catarino, S.O.; Pereira, A.I.; Minas, G.; Pinho, F.T.; Lima, R. Label-free multi-step microfluidic device for mechanical characterization of blood cells: Diabetes type II. *Micro Nano Eng.* **2022**, *16*, 100149. [[CrossRef](#)]
- Dalili, A.; Samiei, E.; Hoorfar, M. A review of sorting, separation and isolation of cells and microbeads for biomedical applications: Microfluidic approaches. *Analyst* **2019**, *144*, 87–113. [[CrossRef](#)] [[PubMed](#)]
- Karimi, A.; Yazdi, S.; Ardekani, A.M. Hydrodynamic mechanisms of cell and particle trapping in microfluidics. *Biomicrofluidics* **2013**, *7*, 021501. [[CrossRef](#)]
- Karimi, S.; Mojaddam, M.; Majidi, S.; Mehrdel, P.; Farré-Lladós, J.; Casals-Terré, J. Numerical and experimental analysis of a high-throughput blood plasma separator for point-of-care applications. *Anal. Bioanal. Chem.* **2021**, *413*, 2867–2878. [[CrossRef](#)]
- Alvankarian, J.; Bahadorimehr, A.; Yeop Majlis, B. A pillar-based microfilter for isolation of white blood cells on elastomeric substrate. *Biomicrofluidics* **2013**, *7*, 14102. [[CrossRef](#)]
- Keskinler, B.; Yildiz, E.; Erhan, E.; Dogru, M.; Bayhan, Y.K.; Akay, G. Crossflow microfiltration of low concentration-nonliving yeast suspensions. *J. Memb. Sci.* **2004**, *233*, 59–69. [[CrossRef](#)]
- Chen, X.; Cui, D.F.; Liu, C.C.; Li, H. Microfluidic chip for blood cell separation and collection based on crossflow filtration. *Sens. Actuators B Chem.* **2008**, *130*, 216–221. [[CrossRef](#)]
- Rodrigues, R.O.; Pinho, D.; Faustino, V.; Lima, R. A simple microfluidic device for the deformability assessment of blood cells in a continuous flow. *Biomed. Microdevices* **2015**, *17*, 108. [[CrossRef](#)] [[PubMed](#)]
- Faustino, V.; Catarino, S.O.; Pinho, D.; Lima, R.A.; Minas, G. A passive microfluidic device based on crossflow filtration for cell separation measurements: A spectrophotometric characterization. *Biosensors* **2018**, *8*, 125. [[CrossRef](#)]
- Faustino, V.; Pinho, D.; Catarino, S.O.; Minas, G.; Lima, R.A. Geometry effect in multi-step crossflow microfluidic devices for red blood cells separation and deformability assessment. *Biomed. Microdevices* **2022**, *24*, 20. [[CrossRef](#)] [[PubMed](#)]
- Laxmi, V.; Joshi, S.S.; Agrawal, A. Biophysical Phenomenon-Based Separation of Platelet-Poor Plasma from Blood. *Ind. Eng. Chem. Res.* **2021**, *60*, 7464–7473. [[CrossRef](#)]
- Liu, S.C.; Yoo, P.B.; Garg, N.; Lee, A.P.; Rasheed, S. A microfluidic device for blood plasma separation and fluorescence detection of biomarkers using acoustic microstreaming. *Sensors Actuators A Phys.* **2021**, *317*, 112482. [[CrossRef](#)]
- Sadek, S.H.; Rubio, M.; Lima, R.; Vega, E.J. Blood Particulate Analogue Fluids: A Review. *Materials* **2021**, *14*, 2451. [[CrossRef](#)] [[PubMed](#)]
- Miranda, I.; Souza, A.; Sousa, P.; Ribeiro, J.; Castanheira, E.M.S.; Lima, R.; Minas, G. Properties and Applications of PDMS for Biomedical Engineering: A Review. *J. Funct. Biomater.* **2021**, *13*, 2. [[CrossRef](#)]

19. Choi, Y.H.; Chung, K.H.; Hong, H.B.; Lee, W.S. Production of PDMS microparticles by emulsification of two phases and their potential biological application. *Int. J. Polym. Mater. Polym. Biomater.* **2017**, *67*, 686–692. [[CrossRef](#)]
20. López, M.; Rubio, M.; Sadek, S.H.; Vega, E.J. A simple emulsification technique for the production of micro-sized flexible powder of polydimethylsiloxane (PDMS). *Powder Technol.* **2020**, *366*, 610–616. [[CrossRef](#)]
21. Lima, R.; Vega, E.J.; Moita, A.S.; Miranda, J.M.; Pinho, D.; Moreira, A.L.N. Fast, flexible and low-cost multiphase blood analogue for biomedical and energy applications. *Exp. Fluids* **2020**, *61*, 231. [[CrossRef](#)]
22. Costa, M.S.; Baptista, V.; Ferreira, G.M.; Lima, D.; Minas, G.; Veiga, M.I.; Catarino, S.O. Multilayer thin-film optical filters for reflectance-based malaria diagnostics. *Micromachines* **2021**, *12*, 890. [[CrossRef](#)] [[PubMed](#)]
23. Lana Rosa, C.; Priscila Oliveira Souza Martins, F.D.E.; Dos Santos Arantes, R.; Mauricio Silva, V.D.A.; Marcel Oliveira, T.; Argolo Saliba, W. Construção De Espectrofotômetro Visível Para Fins Didáticos Construction of Visible Spectrophotometer for Didactic Studies. *J. Exact Sci.* **2019**, *21*, 20–25.
24. Al Khalid, I.; Mohammad, K.S.D.; AlSalhi, M.S.; Prasad, S.; Masilamani, V.; Zuhair, A.-K.I.; Mohammad, K.; Devanesan, S.; AlSalhi, M.S. Shelf-life enhancement of donor blood by He–Ne laser biostimulation. *Curr. Sci.* **2015**, *109*, 1151–1153.
25. Maciel, C.; Fujita, A.; Gueroni, D.I.; Ramos, A.D.; Capurro, M.L.; Sá-Nunes, A. Evans Blue as a Simple Method to Discriminate Mosquitoes' Feeding Choice on Small Laboratory Animals. *PLoS ONE* **2014**, *9*, 1–12. [[CrossRef](#)] [[PubMed](#)]
26. Paul, R.; Zhou, Y.; Nikfar, M.; Razizadeh, M.; Liu, Y. Quantitative absorption imaging of red blood cells to determine physical and mechanical properties. *RSC Adv.* **2020**, *10*, 38923–38936. [[CrossRef](#)] [[PubMed](#)]